IEEE Photonics Journal
An IEEE Photonics Society Publication

GaN-Based Miniaturized Cyan Light-Emitting Diodes on a Patterned Sapphire Substrate With Improved Fiber Coupling for Very High-Speed Plastic Optical Fiber Communication

Volume 4, Number 5, October 2012

Jhih-Min Wun
Che-Wei Lin
Wei Chen
J.-K. Sheu
Ching-Liang Lin
Yun-Li Li
John E. Bowers
Jin-Wei Shi
Juri Vinogradov
Roman Kruglov
Olaf Ziemann

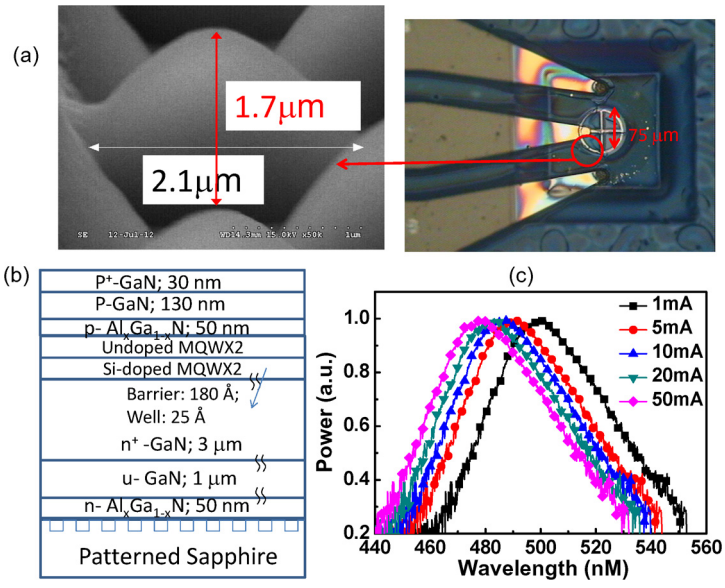

DOI: 10.1109/JPHOT.2012.2210867
1943-0655/$31.00 ©2012 IEEE

GaN-Based Miniaturized Cyan Light-Emitting Diodes on a Patterned Sapphire Substrate With Improved Fiber Coupling for Very High-Speed Plastic Optical Fiber Communication

Jhih-Min Wun,[1] Che-Wei Lin,[1] Wei Chen,[1] J.-K. Sheu,[2] Ching-Liang Lin,[3] Yun-Li Li,[3] John E. Bowers,[4] Jin-Wei Shi,[1] Juri Vinogradov,[5] Roman Kruglov,[5] and Olaf Ziemann[5]

[1]Department of Electrical Engineering, National Central University, Taoyuan 320, Taiwan
[2]Institute of Electro-Optical Science and Engineering, National Cheng-Kung University, Tainan 701, Taiwan
[3]Genesis Photonics Inc., Tainan 741, Taiwan
[4]Electrical and Computer Engineering Department, University of California, Santa Barbara, CA 93106 USA
[5]Polymer Optical Fiber Application Center, Institute of the University of Applied Sciences Nürnberg, 90489 Nürnberg, Germany

DOI: 10.1109/JPHOT.2012.2210867
1943-0655/$31.00 ©2012 IEEE

Manuscript received June 24, 2012; revised July 19, 2012; accepted July 21, 2012. Date of publication July 31, 2012; date of current version August 14, 2012. This work was supported by the National Science Council of Taiwan under Grant NSC-100-2918-I-008-004. Corresponding author: J.-W. Shi (e-mail: jwshi@ee.ncu.edu.tw).

Abstract: We demonstrate the performance of a novel cyan light-emitting diode (LED) on a patterned sapphire (PS) substrate as a light source for plastic optical fiber (POF) communications with the central wavelength at 500 nm. To further enhance the external quantum efficiency (EQE) and output power of this miniaturized high-speed LED, a LED with a PS substrate is adopted. Furthermore, by greatly reducing the number of active $In_xGa_{1-x}N$/GaN multiple quantum wells (MQWs) to four and minimizing the device active area, we can achieve a record-high electrical-to-optical (E–O) bandwidth (as high as 400 MHz) among all the reported high-speed visible LEDs under a very small dc bias current (40 mA). The fiber coupling efficiency has been improved in 4 dB using lens with a 500-μm diameter mounted on the LED chip. Thus, the maximum fiber-coupled power was -2.67 dBm at the bias current of 40 mA. The 1.07-Gb/s data transmissions over a 50-m SI-POF fiber have been successfully demonstrated using this device at the bias current of 40 mA.

Index Terms: Light-emitting diodes, fiber optics communications.

1. Introduction

Recently, high-speed GaAs-based red resonant-cavity (RC) light-emitting diodes (RCLEDs) ($\sim$650 nm) have been used for applications in polymethylmethacrylate (PMMA)-based plastic optical fiber (POF) communication [1]–[4]. Although the technologies for vertical-cavity surface-emitting lasers (VCSELs) at 850 nm [5], [6], which are used for multimode glass-optical-fiber-based short-reach communication [7], [8], become mature and exhibit much faster data rate transmission than that of the RCLEDs used for POF communication, RCLEDs still have niche applications in harsh-environment communication, such as for in-car data transmission [1]–[4] and data

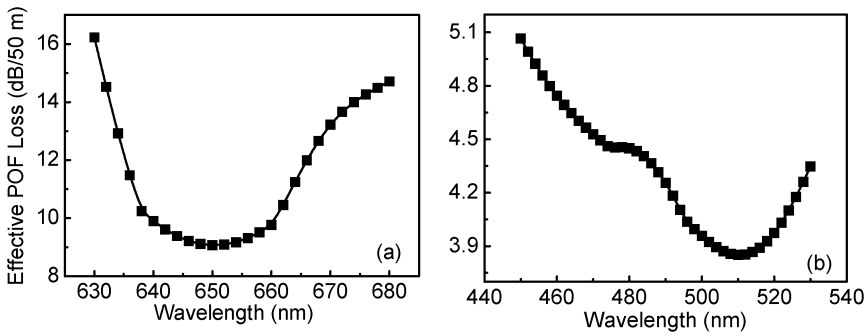

Fig. 1. The measured optical loss spectra of PMMA POFs at red (∼650-nm wavelengths) (a) and blue-green (450–550-nm wavelengths) operating windows.

acquisition/control in power generation systems (e.g., wind farms) [1]–[4], [9]. This is because of its much lower required driving current density than that of the VCSEL, which provides the improved device reliability needed for harsh-environment operation [4]. However, in comparison to PMMA loss window at the wavelength of around 500 nm, the red operating window has a narrower optical bandwidth (∼5 nm versus ∼20 nm) and a higher attenuation (8 dB/50 m versus 4 dB/50 m). Fig. 1(a) and (b) shows the effective spectral loss, which defines the actual attenuation under assumption that the optical source has a Gaussian-shaped spectrum with a full-width at half-maximum (FWHM) of 30 nm. As can be seen, the PMMA-POF link operating with short-wavelength optical sources provides a better performance. Moreover, it has a better tolerance to transmitter with wider spectrum or to spectral drift with temperature.

The suitability of high-speed III-nitride-based green (cyan) or blue LEDs [10]–[16] at around wavelengths of 400–530 nm have thus been demonstrated to meet such applications. Compared with the GaAs-based red RCLEDs, the nitride-based LEDs should be much more immune to variations in ambient temperature and more suitable for communications in a harsh environment due to their larger band gap [14]. In previous reports [14], we demonstrated the invariability of high-speed performance of III-nitride-based green LEDs at ambient temperatures as high as 200 °C.

The other major application of III-nitride-based LEDs is for solid-state lighting. This also drives the development in improving their high-speed performance for white-light indoor wireless communication [16]–[19]. However, the power consumption reported for these III-nitride LEDs for high-speed operation is usually larger than that of red RCLEDs. The bias current required for > 200-Mb/s error-free POF data transmission at room temperature (RT) for the reported green and red LEDs is around 60 mA [14] and ∼30 mA [1]–[4], respectively. In order to achieve a higher modulation speed with lower power consumption for POF data transmission, the III-nitride-based high-speed green laser diodes (LDs) [20] at ∼520-nm wavelength is another attractive choice. Compared with the discussed III-nitride-based green LEDs, the III-nitride-based green LDs should have the potential to offer a larger modulation speed and a higher optical power coupled into the POF. Nevertheless, due to the limited material gain of $In_xGa_{1-x}N$/GaN-based green multiple quantum wells (MQWs), a long LD cavity length (up to ∼1 mm) is thus necessary to overcome mirror loss and have the lasing phenomenon [20], [21]. This would result in a small RC-limited bandwidth and also seriously limit the maximum data rate during POF transmission. Furthermore, a large bias current and an external temperature controller are both necessary to attain a wide electrical-to-optical (E–O) bandwidth (∼1 GHz) for this type of long-cavity laser [20].

In this paper, we demonstrate the performance of a novel high-speed cyan nitride-based LED with a miniaturized device area and thin active region designed to minimize the required bias current for high-speed operation. In order to enhance the external quantum efficiency (EQE) and sustain the output optical power of such a small device for POF communication, it was fabricated on the patterned sapphire (PS) substrate [22]. Under a small dc bias current (∼40 mA), we can achieve a record 3-dB E–O bandwidth as high as 0.4 GHz among all the reported high-speed visible LEDs [1]–[4], [10]–[16]. The lens with a 500-μm diameter mounted on the LED chip improves the coupling

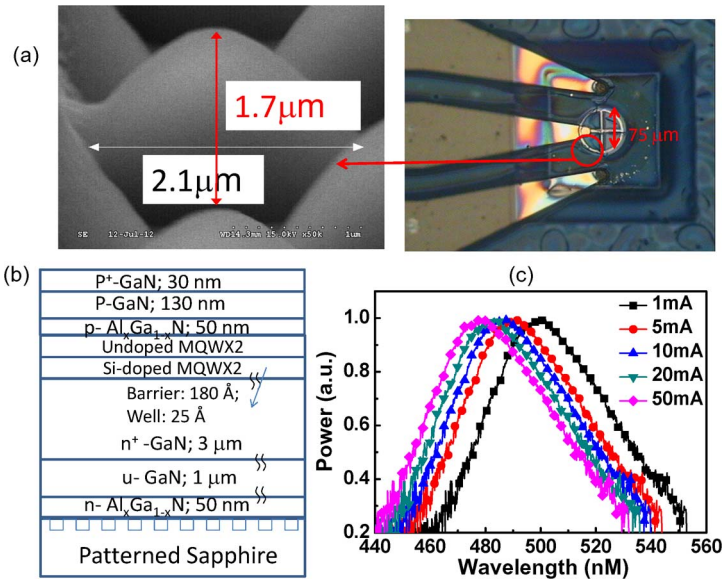

Fig. 2. (a) A top view of the demonstrated LED and the zoom-in SEM picture of the PS substrate. (b) The conceptual cross-sectional view of demonstrated device. (c) The measured electroluminescence spectra of the demonstrated device under different bias currents.

efficiency in ∼4 dB. At the bias current of 40 mA, the fiber-coupled power achieves −2.67 dBm. By using the novel transmitter and Si-based 800-MHz photo-receiver circuits with an 800-μm active diameter, error-free 1.07-Gb/s data transmission over a 50-m POF fiber has been successfully demonstrated.

2. Device Structure and Fabrication

Fig. 2(b) shows a conceptual cross-sectional view of our proposed device structure. The epilayer structures were grown on a (0001) PS substrate. The four-period $In_xGa_{1-x}N$/GaN cyan MQW region, bottom n-type GaN layer, and topmost p-type (Al)GaN layer were about ∼80, 3000, and 210 nm thick, respectively. The thickness of the GaN barrier and InGaN well layers was 180 and 25 Å, respectively. The n-type doping density in the GaN barrier layers of the two MQWs closest to the n-type cladding layer was around 2×10^{18} cm^{-3}. The GaN barrier layers in the other two MQW layers were left undoped. The partial n-type doping profile was used to enhance the modulation speed and output power of the LEDs; see our previous work [12]. Furthermore, our active layer is much thinner (80 versus 200 nm) than that typically reported for high-speed nitride-based green LEDs [10]–[14], which can increase the injected carrier density, shorten the spontaneous recombination time, and enhance the operation speed [23]. Fig. 2(a) shows the top view of the demonstrated LED and a zoom-in scanning electron microscope (SEM) picture of the periodic structures, which have a triangular shape with around 2 μm width and height, on the PS substrate. Each LED has an active diameter of around 50 or 75 μm. During device fabrication, each LED is etched down to the insulating sapphire substrate to minimize the parasitic capacitance of the device. For details of the fabrication processes, please refer to our previous work [12], [14]. The PS substrate cannot only enhance the output light extraction efficiency but also improve the quality of the epilayer structure [22]. These advantages can enhance the output power from the LED for data transmission, improve electrostatic discharge (ESD) endurance voltages, and minimize its leakage current [22], which become especially important when the device active area is further downscaled to attain very high-speed performance. Fig. 2(c) shows the measured electroluminescence spectrum of our device with a 75-μm active diameter under different bias currents. As can be seen, the measured central wavelength (∼500 nm) exactly matches the loss minimum

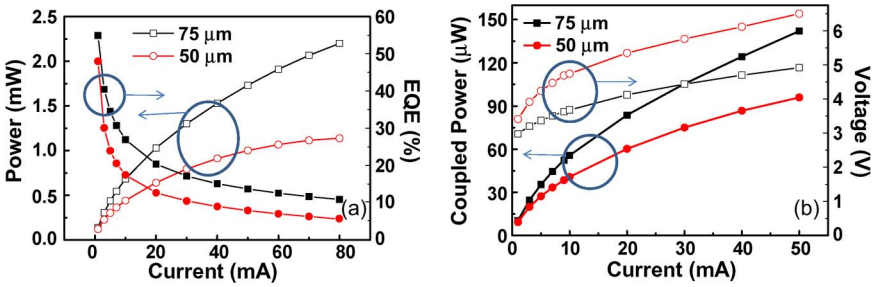

Fig. 3. (a) The measured output optical power (P) and EQE of devices versus the bias current (I). (b) The butt-joint coupled power to POF and corresponding bias voltage versus bias current of device with a 75- and a 50-μm active diameter.

window of standard PMMA POF (< 4 dB/50 m), as shown in Fig. 1. In addition, when the bias current increases from 1 to 50 mA, the measured central wavelength gradually blue shifts from ~500 nm to ~480 nm. This phenomenon is usually observed in III-nitride LEDs and can be attributed to the screening of the piezoelectric (PZ) field inside the active MQW layers by the external injected carriers [24], [25].

3. Measurement Results

Fig. 3(a) shows the total free-space output power (P) and the corresponding EQE from devices with two different active diameters (50 and 75 μm), operated at RT, as measured by the integrating sphere, versus the bias current (I). We can clearly see that, under a moderate bias current density (5 mA, ~200 A/cm^2) [24]–[26], our device exhibits high absolute EQE (~50%) [26], which indicates the benefit of the PS substrate to enhance the light extraction efficiency [22] of our LED. Compared with the reported high-speed green III-nitride-based LEDs [10]–[14], our demonstrated device can have a comparable or higher output power with a much smaller active area and under a lower required bias current. Fig. 3(b) shows the measured I (current)–V (voltage) curves and the coupled power from the 50- and 75-μm devices under different bias currents (at RT) into the standard PMMA-based POF with a 1-mm core diameter. Based on the I–V curves, we can clearly see that the differential resistance measured under a ~70-mA bias current of 50- and 75-μm devices is as low as 29 and 18 Ω, respectively. Such low resistance, combined with the small junction capacitance due to the miniaturized device size, implies a very high RC-limited bandwidth. The modeling results for our device show that the RC-limited bandwidth of both devices is over 4 GHz [24], which is much higher than that of the measured E–O bandwidths, as will be discussed later. On the other hand, by comparing the free-space output power with the coupled power as shown in Fig. 3(a) and (b), respectively, we can extract the butt-joint coupling efficiency, which is around 8% for both devices. Such low values of coupling efficiency should be improved by using a lens, which will be discussed later. The capability for high-temperature operation is also a key issue for harsh-environment communication. Fig. 4(a) and (b) shows the variation in the coupling power into the POF versus the bias current measured under different ambient temperatures (25 °C, 50 °C, 100 °C, and 130 °C). The insets show the difference in output power ($\triangle$p) between RT (25 °C) and high-temperature (50 °C, 100 °C, and 130 °C) operations of devices under different bias currents. These values of power ($\triangle$p) are normalized to the output power of devices ($\triangle$p/p) at corresponding bias currents under RT operation.

As can be seen, for both devices, when the bias current is over ~10 mA, the variation of the output power with the increasing of bias current is minimized. Under 40-mA bias current operation, which corresponds to the required bias current for the maximum 3-dB O–E bandwidth, the degradation in output power is only around 15% for both devices under 100 °C operation. This phenomenon is very different from the behavior of typical semiconductor-based light emitters, which usually exhibit a monotonic increase in the degree of output-power degradation with an increase in the bias current, especially under high-temperature operation, due to the increase in junction

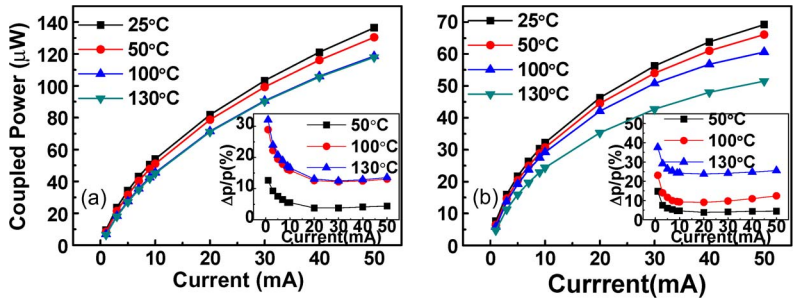

Fig. 4. The measured coupling power versus bias current from (a) the large device (diameter: 75 μm) and (b) the small device (diameter: 50 μm) into the POF under four different ambient temperatures (25 °C, 50 °C, 100 °C, and 130 °C). The insets show the difference in output power after normalization ($\triangle$p/p) between RT (25 °C) and high-temperature (50 °C, 100 °C, and 130 °C) operations of such two devices under different bias currents.

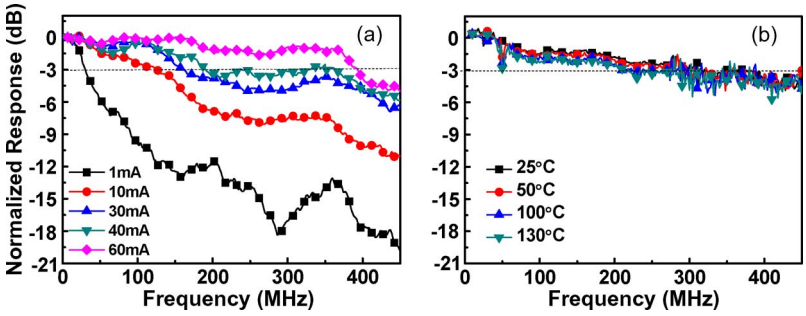

Fig. 5. (a) The measured E–O frequency responses of a 50-μm device under different bias currents, and (b) the measured E–O frequency responses of the same device in (a) under a fixed bias current (50 mA) and different ambient temperatures.

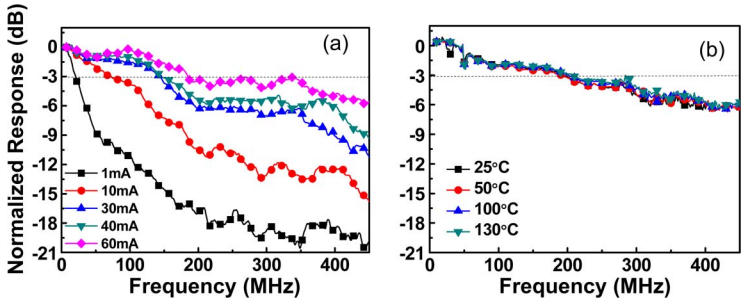

Fig. 6. (a) The measured E–O frequency responses of a 75-μm device under different bias currents, and (b) the measured E–O frequency responses of the same device in (a) under a fixed bias current (50 mA) and different ambient temperatures.

temperature. These static measurement results can be attributed to the influence of the strong PZ field inside the GaN/InGaN MQW region [24], [25]. When the bias current exceeds a certain value ($>$ 10 mA for our case), the PZ field is completely screened, and the effective barrier height in the MQW region thus increases [24], [25]. This should be accompanied by a lower probability of carrier-escape and less output-power degradation under high-temperature operation [24], [25].

Figs. 5(a) and 6(a) show the measured E–O modulation frequency responses of our 50- and 75-μm devices under different bias currents and at RT operation, respectively. As can be seen,

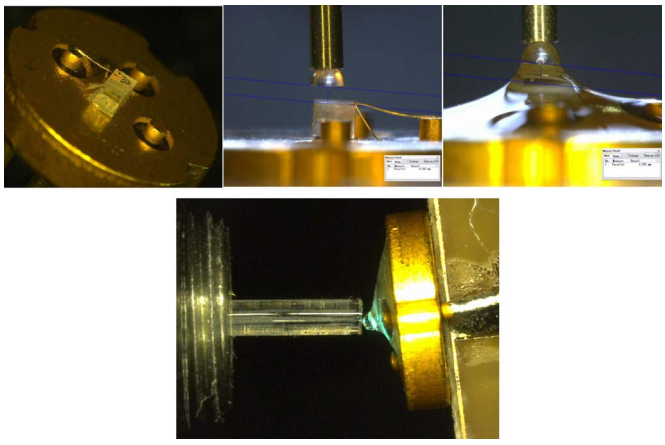

Fig. 7. The photos of the LED chip before and after mounting of the 500-μm glass lens.

when the bias current reaches 40 mA for both devices, the measured 3-dB E–O bandwidth can be as wide as 0.4 and 0.2 GHz, respectively. This measured maximum speed performance of our small device is even faster than that reported for the high-speed red RCLED (350 MHz [1]), which has a much more complex epilayer structure and should have the highest performance ever reported for any visible LEDs [1]–[4], [10]–[15].

In comparison with previously published high-speed green LEDs [12], the thinning of active layers and downscaling of device active area allows achieving a higher modulation speed (400 MHz versus 330 MHz) at lower bias current ($\sim$40 versus 110 mA) [12]. Figs. 5(b) and 6(b) show the measured E–O modulation frequency responses under the fixed bias current of 50 mA and different ambient temperatures (RT to 130 °C). As can be seen, there is no significant bandwidth degradation within the wide temperature range up to 130 °C. This result is rather different from the RCLEDs operating at 650 nm [1], which have a comparable speed performance but, at the same time, demonstrate significant output-power degradation in $\sim$40% at temperature growth from 10 °C to 70 °C [1]. Based on these static and dynamic measurement results, shown in Figs. 4–6, we can conclude that the larger band-gap difference in the active layer can really suppress the carrier leakage from active area of III-nitride LED, offering superior high-temperature performance.

For the further improvement of the coupling efficiency between LED with 75-μm active areas and POF, the lens has been mounted on the LED chip (see Fig. 7). The used ball lens with a radius (R) of 250 μm is made from the material BK7 glass, and its refractive index (n) is 1.57. The estimation for the focal length of a half ball lens is 440 μm (R/(n - 1)). The principal plane is R/n away from the flat surface (160 μm), and the corresponding focal point is about 600 μm away from the LED surface. As shown in Fig. 7, we thus set the ball lens very close to the POF surface. The P–I curves in Fig. 8(a) show the fiber-coupled power measured after 1-m POF using an integration sphere. As can be seen, two traces measured by the use of two different packaged devices, which represent the best and worst measurement results, are shown. In comparison with butt-coupled solution, the lens improved the coupling efficiency, which ranges from 4 to 5 dB. Thus, the maximum fiber-coupled power demonstrated during the test was $-$2.67 dBm at bias current of 40 mA, which is around 36% of the total free-space output power of the device. Such results are comparable with parameters of the commercially available red RCLED designed for 250-Mb/s data transmission with $-$2-dBm fiber-coupled power at the bias current of 45 mA[1].

Fig. 8(b) shows the measured E–O modulation frequency responses of the packaged device with a 75-μm active area diameter. As can be seen, the measured 3-dB bandwidth is around 210 MHz, which is close to its on-wafer measurements (see Fig. 6).

For the data transmission tests, 10- and 50-m SI-POF (class A4a.2) links have been used. The transmission setup includes the LED with a 75-μm active area, which has been driven

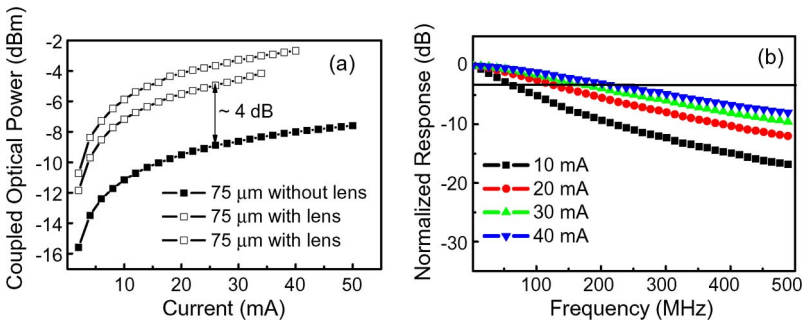

Fig. 8. (a) The fiber-coupled optical power versus bias current of the LED with/without lens. (b) The measured E–O modulation frequency responses of the packaged LED (with lens) under different bias currents.

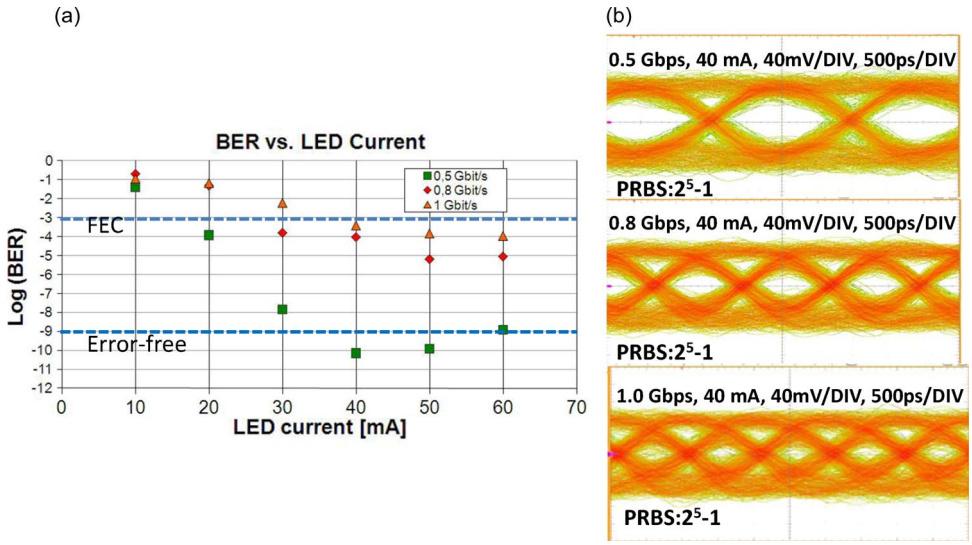

Fig. 9. (a) The measured BER versus bias current of the 75-μm LED (without lens package) with different data rates (0.5, 0.8, and 1 Gb/s); (b) corresponding eye diagrams at the bias current of 40 mA.

over Bias-T in its linear region with peak-to-peak modulation amplitude of 4.5 V; the fiber link of SI-POF Mitsubishi GH4001 with 1-mm core diameter (POF class A4a.2, according IEC 60793-2-40); and an optical receiver based on a 800-μm silicon pin photodiode (Si-PD) HAMAMATSU S5052, which is connected to a transimpedance amplifier (TIA) with 3-dB bandwidth of 800 MHz.

Fig. 9(a) shows the measured bit-error rate (BER) after a 10-m SI-POF link with a passive equalizer depending on bias current of the 75-μm LED without lens. The LED was directly driven with a pseudorandom bit sequence (PRBS $2^5 - 1$) with a bit rate of 0.5, 0.8, and 1.0 Gb/s. The use of a PRBS sequence length of 31 $(2^5 - 1)$ is comparable to a B4B5 coded signal (maximum of five equal symbols). The influence of the low frequency response on PAM16 (pulse-amplitude modulation with 16 discrete levels) and DMT (discrete multitone) modulation, which have a longer PRBS length and a lower symbol rate, is subject for next future investigations. The error-free operation can be achieved for the bit rate of 0.5 Gb/s under the bias current of 40 mA. Fig. 9(b) shows the measured eye patterns for the data rates of 0.5, 0.8, and 1.0 Gb/s. The implementation of the forward error correction coding (FEC) [27] with 7% overhead provides error-free operation of the 10-m SI-POF link at 0.93 Gb/s under the bias current of 40 mA.

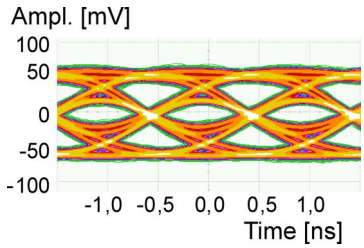

Fig. 10. Eye diagram measured at 1 Gb/s over 10-m SI-POF, which includes a 75-μm LED equipped with a lens, at the bias current of 40 mA.

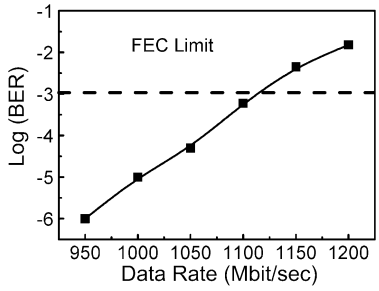

Fig. 11. The measured BER values at different data rates after the 50-m SI-POF transmission link, which includes a 75-μm LED equipped with a lens, at the bias current of 40 mA.

The further improvement of the system performance requires a higher fiber-coupled power. Fig. 10 shows the measured 1-Gb/s eye diagram obtained after the 10-m SI-POF transmission link, which includes 75-μm LED equipped with a lens. The LED with improved coupling efficiency provides a higher optical power at the far end of the system, and thus, we can obtain the 1-Gb/s eye patterns with a better signal-to-noise ratio than that of the eye patterns shown in Fig. 9(b) with the same data rate and under the same bias current (40 mA). Fig. 11 shows the measured BER depending on the bit rate after the 50-m SI-POF transmission link, which includes 75-μm LED equipped with a lens. After deduction of 7% FEC bits, a maximum net bit rate of 1.07 Gb/s is achieved under a 40-mA bias current.

We have also tested the transmission performance of high-performance red RCLED[1] by the use of the same setup and the same length of POF (50 m). The maximum transmission data rate of red RCLED is higher than that of our device ($\sim$1.45 versus 1.1 Gb/s). This is because the chromatic dispersion of our demonstrated cyan LED at 1 Gb/s over POF lengths of 50 m produces a higher penalty, compared with red RCLED. It has a narrower optical linewidth due to the characteristic of RC structure. On the other hand, this dispersion can be compensated by DFE (decision feedback equalizer) for example, and the power budget advantage of the green LED should be much higher than the chromatic dispersion penalty. Nevertheless, the reduction of the spectral width of the demonstrated cyan LED is a task for the next future.

4. Conclusion

We demonstrate a miniaturized GaN-based cyan LED on a PS substrate, which can enhance the EQE performance and sustain a reasonable output power. By thinning the active layer thickness, shrinking the device active area, and using the TO package with a BK-7 lens for enhancing optical coupling into POF, we can achieve a high coupled power into POF (~ -2.67 dBm), high O–E

[1]FDL 300 E, (red RCLED transmitter) delivered by Firecomms Ltd., 2200 Airport Business Park, Cork, Ireland (www.firecomms.com).

bandwidth (210 MHz), and error-free (after FEC) data rate as high as1.07 Gb/s for a 50-m POF transmission under a reasonable small bias current (40 mA). The high-speed performance of the link can be improved by a suitable LED driver, which has output impedance matched with the LED.

References

[1] M. M. Dumitrescu, M. J. Saarinen, M. D. Guina, and M. V. Pessa, "High-speed resonant cavity light-emitting diodes at 650 nm," *IEEE J. Sel. Topics Quantum Electron.*, vol. 8, no. 2, pp. 219–230, Mar./Apr. 2002.

[2] J. D. Lambkin, B. McGarvey, M. OGorman, and T. Moriarty, "RCLEDs for MOST and IDB 1394 automotive applications," in *Proc. 14th Int. Conf. Polym. Opt. Fiber*, Hong Kong, China, 2005.

[3] R. Wirth, B. Mayer, S. Kugler, and K. Streubel, "Fast LEDs for polymer optical fiber communication at 650 nm," *Proc. SPIE*, vol. 6013, pp. 60130F-1–60130F-8, 2005.

[4] J. D. Lambkin, "Resonant cavity light emitting diodes: An enabling technology for plastic fibre communication applications," in *Proc. Int. Conf. Plastic Opt. Fiber*, Yokohama, Japan, Oct. 2010.

[5] P. Moser, W. Hofmann, P. Wolf, J. A. Lott, G. Larisch, A. Payusov, N. N. Ledentsov, and D. Bimberg, "81 fJ/bit energy-to-data ratio of 850 nm vertical-cavity surface-emitting lasers for optical interconnects," *Appl. Phys. Lett.*, vol. 98, no. 23, pp. 231106-1–231106-3, Jun. 2011.

[6] J.-W. Shi, W.-C. Weng, F.-M. Kuo, Y.-J. Yang, S. Pinches, M. Geen, and A. Joel, "High-performance Zn-diffusion 850-nm vertical-cavity surface-emitting lasers with strained InAlGaAs multiple quantum wells," *IEEE Photon. J.*, vol. 2, no. 6, pp. 960–966, Dec. 2010.

[7] C. L. Schow, F. E. Doany, C. Tsang, N. Ruiz, D. Kuchta, C. Patel, R. Horton, J. Knickerbocker, and J. Kash, "300-Gb/s, 24-channel full-duplex, 850-nm CMOS-based optical transceivers," in *Proc. OFC/NFOEC*, San Diego, CA, Feb. 2008, pp. 1–3.

[8] K. Kurata, "High-speed optical transceiver and systems for optical interconnects," in *Proc. OFC/NFOEC*, San Diego, CA, Mar. 2010, pp. 1–3.

[9] B. Luecke, "Plastic optical fiber: Plastic optical fiber steps out of the niche," *Laser Focus World*, vol. 44, pp. 91–95, Apr. 2008.

[10] M. Akhter, P. Maaskant, B. Roycroft, B. Corbett, P. de Mierry, B. Beaumont, and K. Panzer, "200 Mb/s data transmission through 100m of plastic fiber with nitride LEDs," *Electron. Lett.*, vol. 38, no. 23, pp. 1457–1458, Nov. 2002.

[11] J.-W. Shi, H.-Y. Huang, J.-K. Sheu, C.-H. Chen, Y.-S. Wu, and W.-C. Lai, "The improvement in modulation speed of GaN-based light-emitting diode (LED) by use of n-type barrier doping for plastic optical fiber (POF) communication," *IEEE Photon. Technol. Lett.*, vol. 18, no. 15, pp. 1636–1638, Aug. 2006.

[12] J.-W. Shi, J.-K. Sheu, C.-H. Chen, G.-R. Lin, and W.-C. Lai, "High-speed GaN-based green light emitting diodes with partially n-doped active layers and current-confined apertures," *IEEE Electron Device Lett.*, vol. 29, no. 2, pp. 158–160, Feb. 2008.

[13] S.-Y. Huang, R.-H. Horng, J.-W. Shi, H.-C. Kuo, and D.-S. Wuu, "High-performance InGaN-based green resonant-cavity light-emitting diodes for plastic optical fiber applications," *IEEE/OSA J. Lightw. Technol.*, vol. 27, no. 18, pp. 4084–4089, Sep. 2009.

[14] J.-W. Shi, H.-W. Huang, F.-M. Kuo, J.-K. Sheu, W.-C. Lai, and M.L. Lee, "Very-high temperature (200 °C) and high-speed operation of cascade GaN based green light emitting diodes with an InGaN insertion layer," *IEEE Photon. Technol. Lett.*, vol. 22, no. 14, pp. 1033–1035, Jul. 2010.

[15] J.-W. Shi, C.-W. Lin, W. Chen, J. E. Bowers, J.-K. Sheu, C.-L. Lin, Y.-L. Li, J. Vinogradov, and O. Ziemann, "Very high-speed GaN-based cyan light emitting diode on patterned sapphire substrate for 1 Gbps plastic optical fiber communication," in *Proc. OFC*, Los Angele, CA, Mar. 2012, p. JTh2A.18.

[16] J. J. D. McKendry, R. P. Greeen, A. E. Kelly, Z. Gong, B. Guilhabert, D. Massoubre, E. Gu, and M. D. Dawson, "High-speed visible light communications using individual pixels in a micro light-emitting diode array," *IEEE Photon. Technol. Lett.*, vol. 22, no. 18, pp. 1346–1348, Sep. 2010.

[17] T. Komine and M. Nakagawa, "Fundamental analysis for visible-light communication system using LED lights," *IEEE Trans. Consum. Electron.*, vol. 50, no. 1, pp. 100–107, Feb. 2004.

[18] J. Vucic, C. Kottke, S. Nerreter, A. Buttner, K.-D. Langer, and J. W. Walewski, "White light wireless transmission at 200+ Mb/s net data rate by use of discrete-multitone modulation," *IEEE Photon. Technol. Lett.*, vol. 21, no. 20, pp. 1511–1513, Oct. 2009.

[19] J.-W. Shi, C.-C. Chen, C.-K. Wang, C.-S. Lin, J.-K. Sheu, W.-C. Lai, C.-H. Kuo, C.-J. Tun, T.-H. Yang, F.-C. Tsao, and J.-I. Chyi, "Phosphor-free GaN-based transverse junction white light-emitting diodes with re-grown n-type regions," *IEEE Photon. Technol. Lett.*, vol. 20, no. 6, pp. 449–451, Mar. 2008.

[20] R. Kruglov, J. Vinogradov, O. Ziemann, S. Loquai, J. Muller, U. Strau(, and C.-A. Bunge, "Eye-safe data transmission of 1.25 Gbit/s over 100-m SI-POF using green laser diode," *IEEE Photon. Technol. Lett.*, vol. 24, no. 3, pp. 167–169, Feb. 2012.

[21] S. Lutgen, A. Avramescu, T. Lermer, M. Schillgalies, D. Queren, J. Muller, D. Dini, A. Breidenassel, and U. Strauss, "Progress of blue and green InGaN laser diodes," in *Proc. SPIE*, Jan. 2010, vol. 7616, p. 761 60G.

[22] C. H. Jang, J. K. Sheu, S. J. Chang, M. L. Lee, C. C. Yang, S. J. Tu, F. W. Huang, and C. K. Hsu, "Effect of growth pressure of undoped GaN layer on the ESD characteristics of GaN-based LEDs grown on patterned sapphire," *IEEE Photon. Technol. Lett.*, vol. 23, no. 14, pp. 968–970, Jul. 2011.

[23] K. Ikeda, S. Horiuchi, T. Tanaka, and W. Susaki, "Design parameters of frequency response of GaAs–(Ga,Al)As double heterostructure LED's for optical communications," *IEEE Trans. Electron Devices*, vol. ED-24, no. 7, pp. 1001–1005, Jul. 1977.
[24] J.-W. Shi, H.-W. Huang, F.-M. Kuo, W.-C. Lai, M.L. Lee, and J.-K. Sheu, "Investigation of the carrier dynamic in GaN-based cascade green light-emitting-diodes using the very-fast electrical-optical pump-probe technique," *IEEE Trans. Electron Devices*, vol. 58, no. 2, pp. 495–500, Feb. 2011.
[25] J.-W. Shi, F.-M. Kuo, H.-W. Huang, J.-K. Sheu, C.-C. Yang, W.-C. Lai, and M. L. Lee, "The influence of a piezoelectric field on the dynamic performance of GaN-based green light-emitting-diodes with a InGaN insertion layer," *IEEE Electron Device Lett.*, vol. 32, no. 5, pp. 656–658, May 2011.
[26] N. F. Gardner, G. O. Muller, Y. C. Shen, G. Chen, S. Wantanabe, W. Gotz, and M. R. Krames, "Blue-emitting InGaN–GaN double-heterostructure light-emitting diodes reaching maximum quantum efficiency above 200A/cm^2," *Appl. Phys. Lett.*, vol. 91, no. 24, pp. 243506-1–243506-3, Dec. 2007.
[27] B. P. Smith and F. R. Kschischang, "Future prospects for FEC in fiber-optic communications," *IEEE J. Sel. Topics Quantum Electron.*, vol. 16, no. 5, pp. 1245–1257, Sep./Oct. 2010.